Viscosity Dependence of the Local Segmental Dynamics of Anthracene-Labeled Polyisoprene in Dilute Solution

David B. Adolf and M. D. Ediger*

Department of Chemistry, University of Wisconsin—Madison, Madison, Wisconsin 53706

Toshiaki Kitano† and Koichi Ito

Department of Materials Science, Toyohashi University of Technology, Toyohashi 440, Japan

Received June 17, 1991; Revised Manuscript Received September 17, 1991

ABSTRACT: The local segmental dynamics of anthracene-labeled polyisoprene in dilute solution have been studied using time-correlated single photon counting. Nine solvents covering more than 2 decades in viscosity were utilized. The shape of the observed orientation autocorrelation functions was independent of solvent, temperature, and viscosity. Correlation times (τ_c) were determined as a function of temperature in all solvents. Contrary to the prediction of Kramers' theory in the high-friction limit, it was found that $\tau_c \propto \eta^{0.75}$ at constant temperature. An apparent power law dependence was also observed in a recent ^{13}C NMR study of polyisoprene dynamics in dilute solution. These results are consistent with the idea that the friction opposing conformational transitions is frequency dependent.

Introduction

Understanding polymer dynamics in dilute solutions requires an understanding of the role of the solvent. For the large-scale chain motions described by Rouse and Zimm, dynamics scale linearly with the solvent viscosity at constant temperature and solvent quality.[1] Thus, the solvent provides a viscous continuum in which the chain moves. For local polymer motions, which occur on the scale of a few repeat units, the role of the solvent may be more complicated. The coupling between chain motions and solvent motions may occur on such a short length scale and fast time scale that the effect of the solvent on the chain motions cannot be simply represented by the macroscopic viscosity. This has important implications for the high-frequency mechanical properties of polymer solutions.[2,3]

The influence of the solvent on local polymer motions in dilute solutions has been an active area of research.[4,5] Some studies have reported that local dynamics are linearly dependent on solvent viscosity while others have indicated more complicated behavior. Different polymers appear to show different behavior in this regard. This aspect of the literature has been briefly reviewed recently.[5,6]

The present work was motivated most directly by a recent study from our own laboratory. Glowinkowski and co-workers used ^{13}C NMR to study the local dynamics of polyisoprene in 10 solvents across a wide range of viscosities and temperatures.[7] They found that the correlation time for local dynamics scales as the solvent viscosity η to the 0.41 power. These results are consistent with theories which include frequency-dependent components when calculating the friction opposing local motions. The observed nonlinear dependence on the viscosity was sufficiently unusual that we desired to investigate this system with a different experimental technique.

In the present study, time-correlated single photon counting is used to study the local dynamics of anthracene-labeled polyisoprene in nine solvents as a function of temperature. A viscosity range of 0.4–300 cP is investigated. In most respects the results from these optical experiments agree with the NMR results discussed above. We find that, although specific polymer/solvent interactions are not important, Kramers' theory cannot describe the observed dynamics. As in the NMR experiments, a nonlinear dependence of the local dynamics on viscosity is observed. In detail, the dynamics measured by the optical measurements scale as $\eta^{0.75}$ as opposed to the $\eta^{0.41}$ dependence observed in the NMR experiments. The different exponents can be understood in terms of frequency-dependent friction and the presence of the anthracene label in the optical experiments.

Experimental Section

Materials and Sample Preparation. The polyisoprene chains used in this study contain one anthracene chromophore per chain. The anthracene group is covalently bonded essentially in the middle of the chain (see Figure 1). The electronic transition dipole of the anthracene moiety is oriented along the polymer backbone; hence, any movement of the dipole reflects movement of the polymer backbone. The labeled chains were synthesized anionically as described previously.[8] The samples employed had M_n = 104K chains with a polydispersity of 1.09. The chain microstructure is 54% cis, 36% trans, and 10% 3,4-vinyl.

Solutions of the anthracene-labeled polyisoprene chains were prepared in nine solvents. Toluene,[9] cyclohexane,[9] hexadecane,[10] and 1-eicosene[10] are known to be good solvents for polyisoprene. We believe that the others are also good solvents. Toluene, cyclohexane, dodecane, *cis*-decalin, hexadecane, squalane, and dioctyl phthalate were used as received (all ≥99% purity). 1-Eicosene was used as received at 98% purity. Aroclor 1248 (Monsanto Chemical Co., Lot No. KM502) is a mixture of polychlorinated biphenyls with an average of 3.9 chlorine atoms per molecule (48% chlorine by weight). This solvent was used as obtained from Professor J. Schrag's research group; it had been previously filtered.

The optical densities of the polymer solutions at 406 nm were within the range of 0.08–0.15 in a 3-mm cuvette. The corresponding polymer concentration was less than 1 wt %. Since molecular oxygen can quench the fluorescence of the anthracene label, all solutions were subjected to several freeze–pump–thaw cycles to replace molecular oxygen with molecular nitrogen.

Solvent Viscosities. Equations describing the temperature-dependent viscosities of toluene, cyclohexane, *cis*-decalin, hexadecane, squalane, and Aroclor 1248 are given in ref 7. Viscosity data for dodecane,[11] 1-eicosene,[12] and dioctyl phthalate[13] are presented elsewhere. Solvent viscosities at 45 °C and apparent activation energies for viscous flow (E_η) are given in Table I. The

† Current address: Polyplastics Co., Ltd., 973, Miyajima, Fuji-City, Shizuoka-Pref. 416, Japan.

0024-9297/92/2225-0867$03.00/0

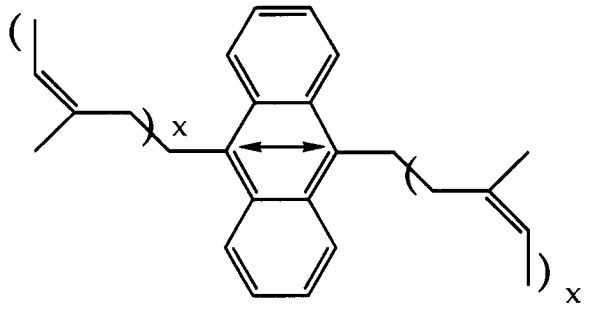

Figure 1. Structure of anthracene-labeled polyisoprene. The $S_0 \rightarrow S_1$ transition dipole is indicated by the double-headed arrow.

Table I
Solvent Characteristics

solvent	η(45 °C), cP	E_η, kJ/mol	E_{exptl}, kJ/mol
toluene	0.44	8.8	16.4
cyclohexane	0.66	12.0	19.2
n-dodecane	1.00	13.0	20.1
cis-decalin	2.05	15.9	20.8
n-hexadecane	2.07	15.0	21.4
1-eicosene	3.40	16.7	23.9
squalane	12.7	32.9	31.8
dioctyl phthalate	19.5	43.9	37.7
Aroclor 1248	34.4	52.5	53.2

E_η values were calculated across the temperature range from 0 to 60 °C, except for cyclohexane, hexadecane, 1-eicosene, and Aroclor 1248. For these four solvents, the bottom of the temperature range was 20, 30, 40, and 35 °C, respectively. The temperature dependence of the viscosity for the three most viscous solvents is not strictly Arrhenius; thus, E_η only gives an approximate indication of the temperature dependence.

Experimental Technique. The method of time-correlated single photon counting was used to observe the local dynamics of the anthracene-labeled polyisoprene. The experimental apparatus, technique,[14] and method of data acquisition have been described elsewhere.[6] Only a brief description will be given here. A 5-ps linearly polarized excitation pulse (406 nm) is used to photoselect an anisotropic distribution of the anthracene labels. Since these chromophores emit light which is polarized along the transition dipole (the double-headed arrow in Figure 1), the fluorescence from the sample is partially polarized until molecular motions randomize the orientation of the excited-state chromophores. Thus, the reorientation of the transition dipole can be observed by monitoring the components of the fluorescence decay polarized parallel and perpendicular to the excitation polarization, $I_\parallel(t)$ and $I_\perp(t)$. The emission wavelength was 414 nm.

The time-dependent anisotropy $r(t)$ can be constructed from $I_\parallel(t)$ and $I_\perp(t)$:

$$r(t) = \frac{I_\parallel(t) - I_\perp(t)}{I_\parallel(t) + 2I_\perp(t)} \tag{1}$$

The anisotropy describes the time dependence of the reorientation of the excited-state chromophores. The decay of the anisotropy is directly related the second-order orientation autocorrelation function

$$r(t) = r(0)\ \mathrm{CF}(t) \tag{2}$$

where $\mathrm{CF}(t)$ is

$$\mathrm{CF}(t) = \langle P_2(\cos\theta\,(t)) \rangle \tag{3}$$

Here P_2 is the second Legendre polynomial and $\theta(t)$ is the angle through which a transition dipole has rotated in time "t" since the excitation pulse. The angular brackets indicate an ensemble average. Thus, the observation of $I_\parallel(t)$ and $I_\perp(t)$ allows the direct calculation of the orientation autocorrelation function without the assumption of any motional model.

Data Analysis. Initially anisotropy decays were fit to the Hall–Helfand model[15] and the generalized diffusion and loss model[16] for the correlation function. It was found that the Hall–Helfand model (HH) gave lower reduced χ^2 values, χ_r^2. Only the fits to the HH function will be used in this paper. The HH equation for the anisotropy is

$$r(t) = r(0)\exp(-t/\tau_1)\exp(-t/\tau_2)\, I_0(t/\tau_1) \tag{4}$$

The quantities $r(0)$, τ_1, and τ_2 are the three fitting parameters. Fits to the HH model typically gave χ_r^2 values <1.3.

The ratio τ_2/τ_1 is determined by the shape of the observed correlation function. This ratio was independent of solvent, viscosity, and temperature, as had been previously observed by Waldow and co-workers.[17] Thus, the mechanism of local dynamics is essentially independent of these factors. In this work, the average value of τ_2/τ_1 was 3.9 with a standard deviation of 1.3. Waldow and co-workers[17] used a holographic grating technique to observe the local dynamics of anthracene-labeled polyisoprene in several low-viscosity solvents. They observed $\tau_2/\tau_1 = 4.4 \pm 1.4$, in good agreement with the current study.

It is convenient to characterize the decay of the anisotropy or correlation function with a single average decay time. We use the correlation time τ_c to do this:

$$\tau_c \equiv \int_0^\infty \mathrm{CF}(t)\, dt \tag{5}$$

In terms of the HH model for the correlation function

$$\tau_c = \left(\frac{1}{\tau_1\tau_2} + \frac{1}{\tau_2^2}\right)^{-1/2} \tag{6}$$

For experiments in which τ_c was less than 85 ns, the decay of the anisotropy was sufficient within the experimental time window for the above procedure to be used. Under these conditions, we believe the error in τ_c to be less than 15%. For two experiments in which the anisotropy decayed more slowly, it was not possible to observe enough of the correlation function to accurately determine its shape (e.g., see the top curve in Figure 2). For these two experiments, the initial slope of the anisotropy decay was used to determine τ_c under the assumption that the ratio of τ_2/τ_1 was in the range observed for the other experiments. The uncertainty in these two τ_c values may be somewhat larger. These points are reported in Figure 3 but are not used in the subsequent analysis of the data.

The fundamental anisotropy $r(0)$ determined by the fitting procedure had an average value of 0.32 with a standard deviation of 0.01. Within experimental uncertainty, this value was independent of solvent, viscosity, and temperature. $r(0)$ is

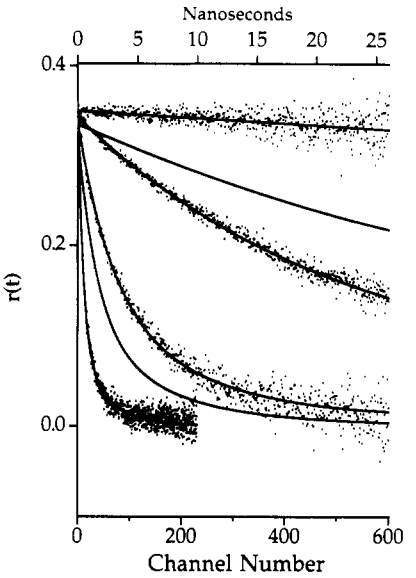

Figure 2. Anisotropy decays for polyisoprene dynamics in six solvents at 0 °C. From top to bottom the solvents and their viscosities are Aroclor 1248 (35 400 cP), dioctyl phthalate (342 cP), squalane (112 cP), *cis*-decalin (5.64 cP), *n*-dodecane (2.28 cP), and toluene (0.77 cP). The dots are experimental data, and the lines are fits to the Hall–Helfand model. Data for dioctyl phthalate and *n*-dodecane have been omitted for clarity.

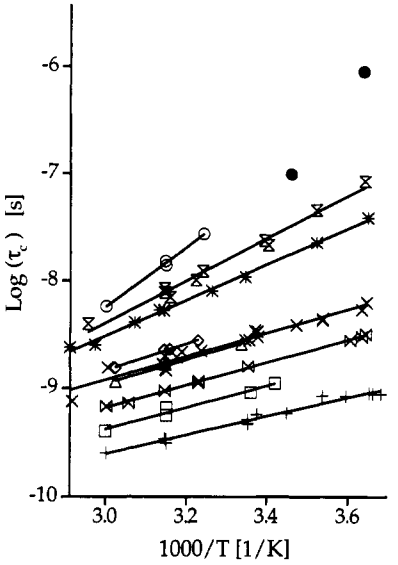

Figure 3. Correlation times for local dynamics of anthracene-labeled polyisoprene. The solvents are (+) toluene, (□) cyclohexane, (⋈) *n*-dodecane, (×) *cis*-decalin, (△) *n*-hexadecane, (◇) 1-eicosene, (*) squalane, (⧖) dioctyl phthalate, (○ and ●) Aroclor 1248. The darkened circles represent experiments where the correlation times have been generated with a constrained fitting method.

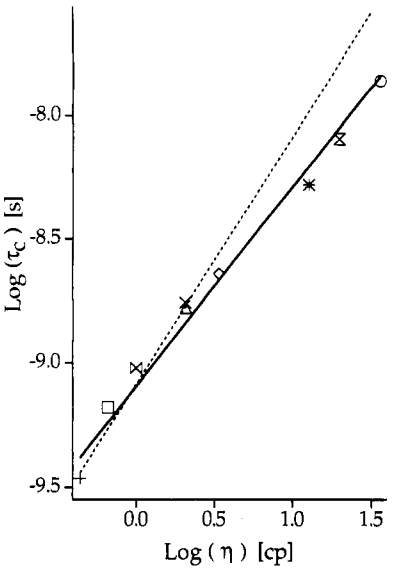

Figure 4. τ_c values at 45 °C as a function of solvent viscosity. The solid line is the best fit line through the points and has a slope of 0.81. The dotted line has a slope of 1.0. The solvent symbols are the same as those for Figure 3.

determined by the polarization of the S_0–S_1 transition moment and should be a constant for a given chromophore. The value of $r(0)$ reported here is in good agreement with a recent study of anthracene-labeled polystyrene in six solvents. Waldow and co-workers[6] reported $r(0) = 0.31 \pm 0.02$ independent of solvent, temperature, and viscosity.

Results

Figure 2 illustrates six representative anisotropy decays for anthracene-labeled polyisoprene. The curves show results in six solvents of varying viscosity at 0 ± 1 °C. The dots are experimental data, and the lines are the best fit of each data set to the HH model. For two of the curves, the data points are not shown. The τ_c values corresponding to these anisotropy decays range from less than 1 ns to more than 100 ns. As discussed in the previous section, the anisotropy decay and τ_c directly characterize the local segmental dynamics of anthracene-labeled polyisoprene. The fastest dynamics occur in toluene, the least viscous solvent. The slowest dynamics occur in Aroclor 1248, the most viscous solvent.

Correlation times for local dynamics in nine solvents over the temperature range of 0–60 °C are plotted in Arrhenius format in Figure 3. The two points with the largest values of τ_c (darkened circles) were generated by the constrained fitting method discussed above. The observed τ_c values span more than 3 decades in range. The experimental activation energies E_{exptl} are obtained directly from the slopes of the lines shown. These values are reported in Table I.

Waldow and co-workers have previously investigated the dynamics of anthracene-labeled polyisoprene in five low-viscosity solvents using a transient holographic grating technique.[17] Where comparisons can be made, the present results are in good agreement with those reported in ref 17. The results they report for 10K labeled chains in cyclohexane and toluene are 19–28% slower than the results for those solvents with 104K labeled chains reported here. Some of this difference can be reasonably attributed to end-over-end motions of the shorter chains. Their results for 304K labeled chains in toluene agree with the results reported here within 3%.

Discussion

Specific Polymer/Solvent Interactions? Many different approaches have been used to discussed the influence of the solvent on local polymer dynamics in dilute solution. Most of these approaches, including the ones discussed in this paper, presuppose that specific polymer/solvent interactions are not important. We believe that this is the case for our results and present two arguments to support this position.

The first argument for the lack of specific polymer/solvent interactions comes from the shape of the observed correlation functions. As discussed in the Experimental Section, these shapes are independent of solvent within experimental error. Since the shape is determined by the detailed mechanism of the local dynamics, this implies that the mechanism of the observed local motions is the same in all solvents studied.

The second argument is based on Figure 4. Here we show the observed τ_c values as a function of solvent viscosity at 45 °C. The full line represents the best fit through the points and has a slope of 0.81. The dotted line has a slope of 1.0, and its significance will be discussed later. Plots analogous to Figure 4 have been constructed every 10 °C between 0 and 60 °C. In each case, the data nearly fall on a straight line. The slopes of these lines fall within the range 0.75 ± 0.06.

It is apparent from these results that, to a good approximation, the correlation time is only a function of solvent viscosity at a given temperature. Specific polymer/solvent interactions would cause deviations from the smooth variation of τ_c with η shown in Figure 4. Note that the solvents used in this study (see Table I) differ considerably in shape, flexibility, and chemical nature, although all are relatively nonpolar.

Two of the solvents dramatically illustrate the extent to which viscosity determines the correlation time. Hexadecane and *cis*-decalin are essentially isoviscous throughout the temperature range studied. As shown in Figure 3, τ_c values in these two solvents are also essentially identical.

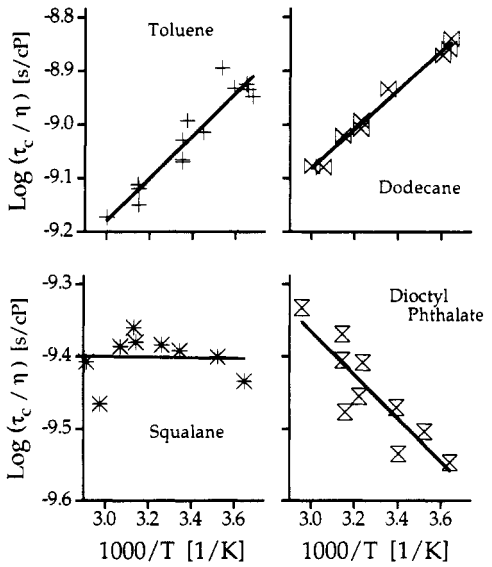

Figure 5. Arrhenius plots of τ_c/η for four solvents. The negative slope for the two bottom panels indicates that Kramers' theory in the high-friction limit cannot describe the data.

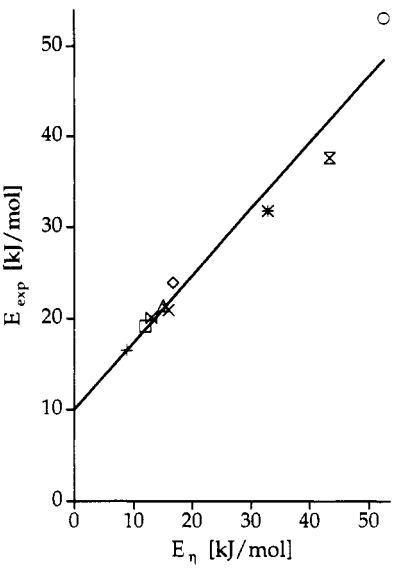

Figure 6. Plot of E_{exptl} vs E_η (eq 11). The best fit line yields $E_a = 10 \pm 1$ kJ/mol and $\alpha = 0.74 \pm 0.07$. The solvent symbols are the same as those for Figure 3.

The lack of specific polymer/solvent interactions implies that we can write τ_c as a function of only solvent η and T:

$$\tau_c = F[\eta(T),T] \tag{7}$$

In the next sections we discuss the nature of the function F and its physical interpretation.

Kramers' Theory. In 1940 Kramers treated the problem of the passage of a particle over a potential energy barrier in the presence of friction (collisions).[18] His result for the observed transition rate can be written:[19]

$$k_{obs} = \left(\frac{A}{\zeta}\right)\left[\frac{1}{2} + \left(\frac{1}{4} + \frac{m\gamma}{\zeta^2}\right)^{1/2}\right]^{-1} \exp(-E_a/RT) \tag{8}$$

Here ζ is the friction, E_a is the height of the barrier, γ is the curvature of the potential barrier near the top, m is the particle mass, and A is a constant which depends only on the shape of the potential. This treatment has been applied to conformational transitions in polymers by Helfand and co-workers.[19,20] Similar expressions result, with m and ζ applying to the moving section of the polymer chain.

In the limit of high friction, Kramers' expression simplifies considerably. If we assume that friction is directly proportional to the solvent viscosity, that the viscosity is high, and that τ_c is inversely proportional to k_{obs}, we obtain

$$\tau_c \propto \eta^1 \exp(E_a/RT) \tag{9}$$

It is clear that eq 9 cannot describe our results. This equation indicates that τ_c should scale linearly with viscosity at constant temperature. Figure 4 shows clearly that this is not the case. If eq 9 fit the data, the experimental results should follow the dashed line with slope 1.0. The high-friction expression fails more dramatically when data in a single solvent are considered as a function of temperature. According to eq 9, a plot of log (τ_c/η) vs $1/T$ should yield a straight line with a slope determined by E_a. Figure 5 shows such plots for four different solvents. The barrier heights calculated from eq 9 are 8, 7, −1, and −6 kJ/mol. Clearly negative barrier heights are nonphysical and indicate that the high-friction limit of Kramers' equation is not appropriate.

We now consider whether the general Kramers expression (eq 8) can describe our experimental results. There are two arguments that indicate that it cannot, as long as a linear relationship is assumed between the friction and the viscosity. First, any reasonable estimation of the parameters in eq 8 indicates that the high-friction limit should apply. For example, Pastor and Karplus[21] have conducted computer simulations on butane. Their results indicate that conformational transitions in butane can be considered to be within the high-friction regime of Kramers' equation if the solvent viscosity is greater than 0.8 cP. Almost all our results are for higher viscosities than this. In addition, because of the larger unit involved in conformational transitions, a polymer chain should reach the high-friction limit at even lower viscosities than does butane. Differences between the potential energy surfaces for butane and polyisoprene should not be so great as to invalidate this comparison.

There is a second argument against the applicability of eq 8. There is no choice of parameters in this equation which reproduces the experimental results even if the range of parameters extends to unrealistic values. This point will be discussed further in conjunction with Figure 8.

Relation to Isomerization of Small Molecules. In the discussion of Figure 4, we noted that there is an apparent power law relationship between τ_c and the solvent viscosity. This is similar to results obtained by a number of investigators studying the isomerization of small molecules.[22,23] Note that a conformational transition in a polymer chain can be viewed as an isomerization process.[24]

Fleming and co-workers[23] have suggested that the isomerization rate constant be written as a power law in the viscosity. In terms of the correlation time

$$\tau_c \propto [\eta(T)]^\alpha \exp(E_a/RT) \tag{10}$$

A consequence of this equation is the following relation between the experimental activation energy and the potential barrier height:

$$E_{exptl} = E_a + \alpha E_\eta \tag{11}$$

Figures 6–8 test how well eqs 10 and 11 fit our results. Figure 6 shows a plot of eq 11. The best line through the data points yields $E_a = 10 \pm 1$ kJ/mol and $\alpha = 0.74 \pm 0.07$. This value of α is in good agreement with the values of 0.75 ± 0.06 obtained from the dependence of τ_c on η at

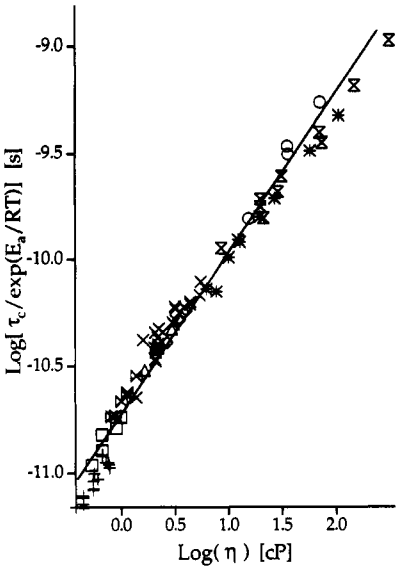

Figure 7. Master plot based on eq 10. The best fit line yields $\alpha = 0.76$. The solvent symbols are the same as those for Figure 3.

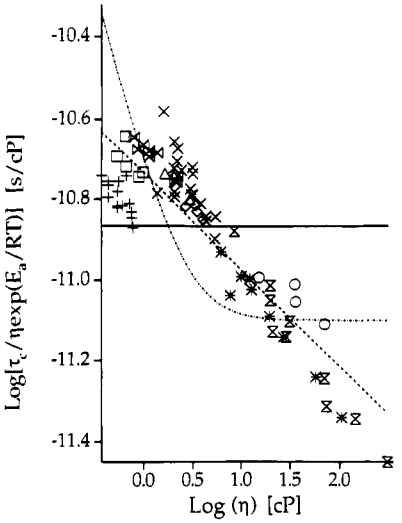

Figure 8. Comparison of experimental results to the predictions of Kramers' theory and eq 10. The dot-dashed curved line is the best fit to the full Kramers expression (eq 8) whereas the straight solid line is the best fit to Kramers' prediction in the high-friction limit. The straight dashed line is a fit to eq 10. The solvent symbols are the same as those for Figure 3.

constant temperature (Figure 4 and similar plots at other temperatures).

Figure 7 shows all the data in a master plot suggested by eq 10 (E_a is taken to be 10 kJ/mol). The data fit a straight line reasonably well, indicating that our results fit eq 10 to a good approximation. The slope of the line gives $\alpha = 0.76$ in agreement with the estimates of α above.

In Figure 8, we compare the three principal models discussed in this paper to the experimental results. The results are plotted such that Kramers' equation in the high-friction limit is a straight, horizontal line (full line). E_a is taken to be 10 kJ/mol. Since almost all of the viscosity and temperature dependence is removed by this plot, small deviations in the data are accentuated. The straight dashed line is a fit to eq 10 with $\alpha = 0.76$ and a proportionality factor of 1.9×10^{-11} s/cP$^{\alpha}$. The dot-dash curve is the best fit to the general Kramers expression (eq 8).[25] Clearly the power law expression shown by the dashed line best represents the results. The two Kramers expressions do not capture even the qualitative features of the data.

We should note that the power law form (eq 10) only approximately fits the experimental results. The deviations of the data from the dashed line shown in Figure 8 (up to 60%) do not represent random experimental error (15%). Small systematic deviations are also present in Figures 4 and 7.

Frequency-Dependent Friction. In this section we discuss a physical interpretation of the apparent power law dependence of the experimental τ_c values upon the solvent viscosity (eq 10). Grote and Hynes[26] have generalized Kramers' theory by allowing the friction ζ to be frequency dependent at very high frequencies. This is in contrast to the usual assumption that ζ is simply proportional to the zero-frequency shear viscosity of the solvent. Grote and Hynes have shown that the friction coefficient applicable to a particular chemical reaction can be much smaller than the friction coefficient calculated from the zero-frequency shear viscosity. To appreciate this result qualitatively, we need to understand that there are two important time scales in this problem. One is τ_c, roughly the average residence time in one well. The other time is the time required to get across the top of the barrier; this time is much smaller than τ_c. If the critical barrier crossing motion is very fast (perhaps 1 ps or less), many of the low-frequency solvent motions which contribute to the zero-frequency shear viscosity will be too slow to affect the reactive motion. If the reactive motion occurs more slowly, the low-frequency (frequency-independent) friction will be adequate to describe the dynamics.

Bagchi and Oxtoby[27] have applied the Grote–Hynes theory to describe the isomerization of stilbene in *n*-alkanes. They found isomerization rates which have a power law dependence on the viscosity, in agreement with eq 10. Thus, it is plausible that the results presented here indicate the importance of frequency-dependent friction in the conformational transitions of polymers. Other possible explanations for the nonlinear dependence of the correlation time on viscosity have also been presented.[28,29] Reference 7 compares some of these alternative explanations.

Comparison to Other Work. The previous paragraphs show that the functional form of the our results is consistent with the idea that frequency-dependent friction is responsible for the observed nonlinear viscosity dependence. We return now to the question posed in the Introduction and compare these results with ^{13}C NMR experiments on the same system. Glowinkowski and coworkers studied the local dynamics of polyisoprene in 10 solvents as a function of temperature.[7] They also found that their results were consistent with eq 10, although with parameters of $E_a = 13 \pm 2$ kJ/mol and $\alpha = 0.41 \pm 0.02$. In the present work $E_a = 10 \pm 1$ kJ/mol and $\alpha = 0.75 \pm 0.06$.

We should keep in mind that the optical experiments measure the dynamics of *anthracene-labeled* polyisoprene. Although the anthracene is present at very low concentration, the optical measurement always senses chain motions in the vicinity of the anthracene chromophore. The difference in E_a observed by the two experiments is fairly small and may well be related to a modification of the potential energy surface in the vicinity of the chromophore.

The difference in the values for α for the two experiments is more substantial. This difference can be qualitatively understood with the context of frequency-dependent friction. The exponent α depends on the moment of inertia and size of the isomerizing unit and on the curvature of

the potential energy surface at the top of the barrier.[27] Larger size, a larger moment of inertia, and a lower barrier all lead to a larger value of α (up to a limit of 1). These factors all lengthen the time required to get across the top of the barrier. When this time is longer, the high-frequency behavior of the friction is less significant and a result closer to Kramers' high-friction limit should be observed. Because of the size of the anthracene chromophore, it is expected that the motions of the labeled chain will involve a larger isomerizing unit and a larger moment of inertia than those of the unlabeled chain. In addition, E_a is slightly lower for the labeled chains. All these factors are consistent with the larger α observed in the optical experiment.

Another interesting comparison can be made with recent work by Waldow and co-workers.[6] They used time-correlated single photon counting to study the local dynamics of anthracene-labeled polystyrene in six solvents as a function of temperature. A wide range of viscosities was also utilized in this study. Waldow and co-workers found that their results were almost consistent with Kramers' equation in the high-friction limit (eq 9). They observed τ_c values proportional to $\eta^{0.90\pm0.05}$. The larger value of α observed for labeled polystyrene in comparison to labeled polyisoprene is likely caused by the bulky side groups of polystyrene. The volume of the isomerizing unit of polystyrene is presumably considerably larger than that for polyisoprene. Thus, the barrier crossing frequency should be lower and α should be closer to 1.

Finally we note that Lee and co-workers have recently proposed an extended Kramers' theory.[30] They have shown that their theory fits small-molecule isomerization data quite well. We have attempted to fit our results to this theory without success. It may be that this difference is due to the large viscosity range covered in the present work. The form proposed by ref 30 predicts a saturation of relaxation times at large viscosities. Our results do not seem to indicate any such saturation.

Summary

The local dynamics of anthracene-labeled polyisoprene have been studied as a function of temperature in nine solvents spanning more than 2 decades in viscosity. Time-correlated single photon counting provides a convenient method of directly monitoring these dynamics from a few hundred picoseconds to almost 100 ns. Consistent with a recent ^{13}C NMR study on polyisoprene, Kramers' theory could not describe the results even though specific polymer/solvent interactions were shown to be unimportant. An apparent power law relationship between the correlation time and the solvent viscosity was observed, with τ_c proportional to $\eta^{0.75}$. Results from the NMR study were also of this form with a somewhat smaller exponent. This nonlinear viscosity dependence is consistent with recent theoretical studies of isomerization dynamics in a medium where the friction is frequency dependent.

This paper and the related NMR study challenge the notion that solvent motions and polymer motions always occur on well-separated time scales. Critical motions near the top of the potential energy barrier for a conformational transition occur on the same time scale as solvent relaxation. Thus, for local motions in dynamically flexible polymers such as polyisoprene, the solvent cannot be treated as a viscous continuum. In these systems, the relaxation of the solvent is intimately related to the relaxation of small segments of the chain.

Acknowledgment. This research was supported by the National Science Foundation: Division of Materials Research, Polymers Program (Grant DMR-8822076), and Chemistry Division, Chemical Instrumentation (Grant CHE-8804083). D.B.A. thanks the Rubber Division of the American Chemical Society for fellowship support. M.D.E. thanks the Alfred P. Sloan Foundation for fellowship support.

References and Notes

(1) Ferry, J. *Viscoelastic Properties of Polymers*, 3rd ed.; Wiley: New York, 1980.
(2) Amelar, S.; Krahn, J. R.; Hermann, K. C.; Morris, R. L.; Lodge, T. P. *Spectrochim. Acta Rev.*, in press.
(3) Gisser, D. J.; Ediger, M. D., submitted for publication in *Macromolecules*.
(4) Mashimo, S. *Macromolecules* **1976**, *9*, 91. Valeur, B.; Monnerie, L. J. *J. Polym. Sci., Polym. Phys. Ed.* **1976**, *14*, 11. Sasaki, T.; Yamamoto, M.; Nishijima, Y. *Macromolecules* **1988**, *21*, 610. Lang, M. C.; Laupretre, F.; Noel, C.; Monnerie, L. J. *J. Chem. Soc., Faraday Trans. 2* **1979**, *75*, 349.
(5) Ediger, M. D. *Annu. Rev. Phys. Chem.*, in press.
(6) Waldow, D. A.; Ediger, M. D.; Yamaguchi, Y.; Matsushita, Y.; Noda, I. *Macromolecules* **1991**, *24*, 3147.
(7) Glowinkowski, S.; Gisser, D. J.; Ediger, M. D. *Macromolecules* **1990**, *23*, 3520.
(8) Hyde, P. D.; Waldow, D. A.; Ediger, M. D.; Kitano, T.; Ito, K. *Macromolecules* **1986**, *19*, 2533.
(9) Brandrup, J., Immergut, E. H., Eds. *Polymer Handbook*, 2nd ed.; Wiley: New York, 1975.
(10) Adachi, K.; Imanishi, Y.; Shinkako, T.; Kotaka, T. *Macromolecules* **1989**, *22*, 2391.
(11) Viswanath, D. S.; Natarajan, G. *Data Book on the Viscosity of Liquids*; Hemisphere Publishing: New York, 1989.
(12) Rossini, F. D. *Selected Values of Physical and Thermodynamic Properties of Hydrocarbons and Related Compounds*; Carnegie Press: Pittsburgh, PA, 1953.
(13) Barlow, A. J.; Lamb, J.; Matheson, A. J. *Proc. R. Soc. London A* **1966**, *292*, 322.
(14) O'Connor, D. V.; Phillips, D. *Time-Correlated Single Photon Counting*; Academic Press: New York, 1984.
(15) Hall, C. K.; Helfand, E. J. *J. Chem. Phys.* **1982**, *77*, 3275.
(16) Viovy, J. L.; Monnerie, L.; Brochon, J. C. *Macromolecules* **1983**, *16*, 1845.
(17) Waldow, D. A.; Johnson, B. S.; Hyde, P. D.; Ediger, M. D.; Kitano, T.; Ito, K. *Macromolecules* **1989**, *22*, 1345.
(18) Kramers, H. A. *Physica* **1940**, *7*, 284.
(19) Helfand, E. *J. Chem. Phys.* **1971**, *54*, 4651.
(20) Skolnick, J.; Helfand, E. *J. Chem. Phys.* **1980**, *72*, 5489. Skolnick, J. *Macromolecules* **1981**, *14*, 646. Helfand, E.; Skolnick, J. *J. Chem. Phys.* **1982**, *77*, 5714.
(21) Pastor, R. W.; Karplus, M. *J. Chem. Phys.* **1989**, *91*, 211.
(22) Flom, S. R.; Nagarajan, V.; Barbara, P. F. *J. Phys. Chem.* **1986**, *90*, 2085. Brearley, A. M.; Flom, S. R.; Nagarajan, V.; Barbara, P. F. *J. Phys. Chem.* **1986**, *90*, 2092.
(23) Courtney, S. H.; Fleming, G. R. *J. Chem. Phys.* **1985**, *83*, 215. Velsko, S. P.; Fleming, G. R. *J. Chem. Phys.* **1982**, *76*, 3553. Keery, K. M.; Fleming, G. R. *Chem. Phys. Lett.* **1982**, *93*, 322.
(24) Liao, T.-P.; Morawetz, H. *Macromolecules* **1980**, *13*, 1228.
(25) The fitting was performed with two free parameters after setting $\zeta = B\eta$ and $\tau_c = C/k_{obs}$. The dash-dot curve shown has $CB/A = 7.9 \times 10^{-12}$ s/cP and $m\gamma/B^2 = 4.0$.
(26) Grote, R. F.; Hynes, J. T. *J. Chem. Phys.* **1980**, *73*, 2715.
(27) Bagchi, B.; Oxtoby, D. W. *J. Chem. Phys.* **1983**, *78*, 2735.
(28) Park, N. S.; Waldeck, D. H. *J. Chem. Phys.* **1989**, *91*, 943.
(29) Nitzan, A. *Adv. Chem. Phys.* **1988**, *70*, 489.
(30) Lee, J.; Zhu, S.-B.; Robinson, G. W. *J. Phys. Chem.* **1987**, *91*, 4273.

Registry No. Polyisoprene, 9003-31-0; toluene, 108-88-3; cyclohexane, 110-82-7; *n*-dodecane, 112-40-3; *cis*-decalin, 493-01-6; *n*-hexadecane, 544-76-3; 1-eicosene, 3452-07-1; squalane, 111-01-3; dioctyl phthalate, 117-81-7; Aroclor 1248, 12672-29-6.